Block Adaptive Quantization of Magellan SAR Data

RONALD KWOK, MEMBER, IEEE, AND WILLIAM T. K. JOHNSON

Abstract—**This paper reports on a data compression scheme which will be used to reduce the SAR data rate on the U.S. NASA Magellan (MGN) mission to Venus. The MGN spacecraft has only one scientific instrument: A radar system used for imaging the surface, for altimetric profiling of the planet topography, and for measuring radiation of the planet surface. A straightforward implementation of the scientific requirements of the mission results in a data rate higher than can be accommodated by the available system bandwidth. A data-rate reduction scheme which includes operation of the radar in burst mode and block adaptive quantization of the SAR data is selected to satisfy the scientific requirements. Descriptions of the quantization scheme and its hardware implementation is given here. Burst-mode SAR operation is also briefly discussed.**

I. Introduction

FOR the Magellan (formerly Venus Radar Mapper—VRM) mission the communication channel to Earth has a limited channel capacity. This limitation requires the output of the Synthetic Aperture Radar (SAR) to be encoded in order to reduce the data rate. The MGN Block Adaptive Quantizer (BAQ) provides a novel approach for encoding the SAR data and establishing the required data rate. The SAR produces 8-bit inphase (I) and quadrature (Q) data samples that are reduced to the required data rate of 2 bits per I and Q plus a small amount of information used for decoding on the ground. Lipes and Butman [1] and Joo and Held [2] have studied compression of raw SAR data with different quantization levels. Comparisons of image data quality using 8-bit and 2-bit quantization have shown that a 2-bit quantizer produces data of acceptable visual quality. However, for inputs with a large dynamic range the distortion due to a quantization to 2 bits severely degrades the amplitude resolution unless the quantization process adapts to the level of the input signals. The adaptation process described in this paper establishes the quantization levels at those appropriate for the observed signal levels and statistics. The design and implementation of this adaptive process and the nonuniform quantizer for the MGN radar are given here. An overview of the Venus mission is given in Section II. Section III describes the data-collection mode employed by MGN. Section IV contains the analysis and design of the BAQ. The implementation of the SAR in hardware is shown in Section V. Simulation results using this quantization scheme are provided in Section VI. Finally, a summary is provided in Section VII.

Manuscript received November 25, 1987; revised February 9, 1989. This work was performed at the Jet Propulsion Laboratory, California Institute of Technology under contract with the National Aeronautics and Space Administration.

The authors are with the Jet Propulsion Laboratory, California Institute of Technology, 4800 Oak Grove Drive, Pasadena, CA 91109.

IEEE Log Number 8928234.

II. Magellan Mission to Venus

Venus is the planet which most closely resembles the Earth in the Solar System. Despite this fact and the great interest shown in the planet by both the U.S. and the USSR, Venus remains a relative mystery due to the optically dense atmosphere which surrounds it. In addition to Earth-based radar studies, the U.S. has sent two missions (the Pioneer Venus Orbiter and Pioneer Venus Multiprobe) and three flyby missions (Mariners 2, 5, and 10), while the USSR has sent several probes, orbiters, and landers (Veneras 4–16 and recently, Vegas I and II). Venera 15/16 employed Synthetic Aperture Radar (SAR) to map about 25 percent of the planet's surface to a resolution of 1–2 km. The Venera 15/16 data, along with Earth-based radar data, have given the best view of the global geology of the planet. Each step toward higher resolution and greater surface coverage has given a better understanding of planetary evolution.

Magellan is scheduled for launching by NASA in April 1989 to acquire data of the planet surface to a resolution of about a factor of ten better than those acquired by Venera 15/16. The scientific objectives are to improve the knowledge of the tectonics and geologic history of Venus by analysis of the surface morphology; the geophysics of Venus, principally its density and distribution; and the small-scale surface physics. To meet these objectives the scientific requirements on the radar system are to produce contiguous images of at least 70 percent of the planet surface with a radar resolution better than 300 m; a surface brightness temperature of the imaged area with a resolution of better than 2 K; and topographic and scattering characteristics maps with a height resolution of better than 50 m.

The radar system is the only scientific instrument on board, and the SAR function will share the 3.7-m diameter antenna with the telecommunications system. A single antenna for these systems requires that all radar data be recorded during the low-altitude portion of the orbit and be down-linked to Earth later on that same orbit in order for the tape recorders to be free to record the next mapping pass. Fig. 1 shows the mapping strategy. A combination of factors led to the selection of a 3.15-h orbit period with a periapsis altitude of 250 km and an apoapsis altitude of 8000 km [3]–[6]. The orbit of 189 min is divided into 37 min of radar data recording, 114 min of playback, and the balance for star sightings and spacecraft

0196-2892/89/0700-0375$01.00 © 1989 IEEE

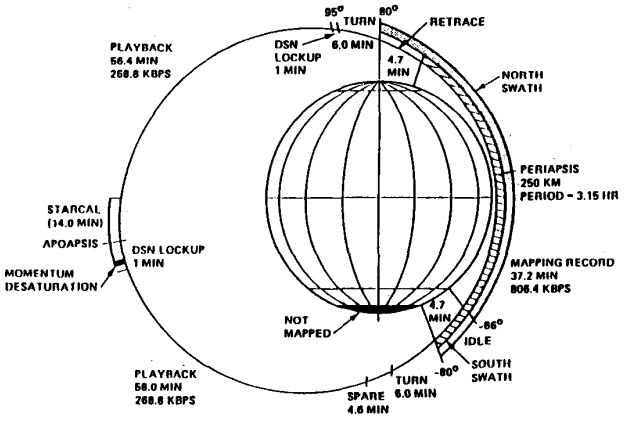

Fig. 1. MGN mapping strategy. The orbit of Magellan is divided into distinct phases. The radar maps the surface when it is closest to Venus. When the mapping pass is completed the antenna is turned towards Earth so that data can be transmitted. After transmission, the antenna is turned back towards the planet for the next mapping pass.

maneuvers. The recorded data is transmitted during the playback part of the orbit. The radar data is recorded at about 806 kbps (kilobits per second) which the system must use in the most efficient manner in order to satisfy the scientific objectives. To satisfy this data-rate constraint the SAR will be operated in the burst mode (discussed in Section III) and the data will be quantized via a data-compression scheme which is the subject of this paper.

Detailed descriptions of SAR imaging could be found in [7]–[9]. A brief explanation of the SAR-image parameters, used throughout this paper, follows. The quality of SAR images is usually described by five parameters: Number of looks, spatial resolution, sidelobe levels, amplitude resolution, signal-to-noise ratio (SNR), and incidence angle. These parameters are not independent and a balance must be achieved in a radar design. The speckle noise inherent in the SAR imagery is reduced by the incoherent averaging of multiple independent-pixel samples derived over several looks [7]. The incidence angle is a view angle and governs the appearance of the image. Usually, incidence angles of 20° or higher produce interpretable images. The system SNR is the signal-to-total noise in the system: this parameter includes thermal noise, ambiguities, quantization noise, and link-error noise. The amplitude resolution is mainly determined by the quantizer. The characteristics and performance of the MGN radar are summarized in Tables I and II.

TABLE I
MAJOR RADAR SYSTEM PARAMETERS

Parameter	Value
SAR	
Operating Altitude	250 to 3500 km
Radar Frequency	2385 MHz
System Bandwidth	2.26 MHz
Antenna Diameter	3.7 m
Antenna Look Angle	10 to 50 deg. (from vertical)
Antenna Gain	36.0dB
Polarization	HH
Transmitted Pulse Length	26.5 usec
Time-bandwidth Product	60
Pulse Repetition Frequency	4420 to 5880 Hz
SAR Burst on Time	25 ms to 250 ms
Transmitted Peak Power	350 W
Average Data Rate (to spacecraft)	750 Kbps

TABLE II
MGN SAR PERFORMANCE

ALTITUDE (Km)	LATITUDE (deg)	INCIDENCE ANGLE(deg)	RANGE RES(m)	AZIMUTH RES(m)	LOOKS NO.
250	+10	52	110	120	4
275	+20, 0	50	113	120	4
500	+40, -20	39	137	120	5
1000	+62, -41	28	182	120	10
1750	+82, -61	21	246	120	10
2100	+90, -68	19	270	120	13

III. MGN SAR Data Collection

For MGN the transmitted carrier is phase-modulated by a 60-bit-long binary sequence or "code" with a pulse width of 26.5 μs. The range bandwidth due to the code is 2.26 MHz. The Doppler bandwidth is determined by the relative motion of the spacecraft and the planet and therefore varies over the orbit. Because of the range and azimuth bandwidths required for high-resolution imaging, the sampling of the data in range and azimuth contributes to a high data rate. This rate must be reduced to satisfy the fixed data rate constraint imposed by the capabilities of the MGN data recorder. The instantaneous data rate is estimated as the product of the sampling and quantizer rate. The sampling rate, the rate of sampling of the I and Q signals (measured in samples/s), is determined by the data-collection scheme. The quantizer rate, which is measured in bits/sample, is fixed by the Block Adaptive Quantizer (BAQ). The quantizer provides for a rate of 2 bits per I and Q data sample.

MGN radar also employs a burst-mode data collection scheme to reduce the data rate. Burst mode is a time-domain data reduction method where the radar does not operate continuously (Fig. 2 illustrates a typical MGN burst cycle). Within a burst cycle, the SAR operates first, followed by the altimeter and radiometer. In this manner the hardware can operate in different modes. For the SAR, a target is illuminated for a fraction of the full-aperture duration of a conventional SAR. The burst-on time, therefore, determines the azimuth resolution, and the number of the bursts during the full-aperture duration determines the number of looks (see Table II). This mode of operation offers a reduction in the data rate but degrades the achievable azimuth resolution compared to the processing of the full aperture. However, the resolution specification can still be met since the achievable resolution of a full aperture is much better than the scientific requirement.

The MGN radar acquires data at an instantaneous rate of about 36 Mbps, which must be reduced to 0.8 Mbps (for recording), a factor of 45 reduction, without severely degrading the resulting image quality. This reduction factor is obtained as follows: 1) The echo data is buffered

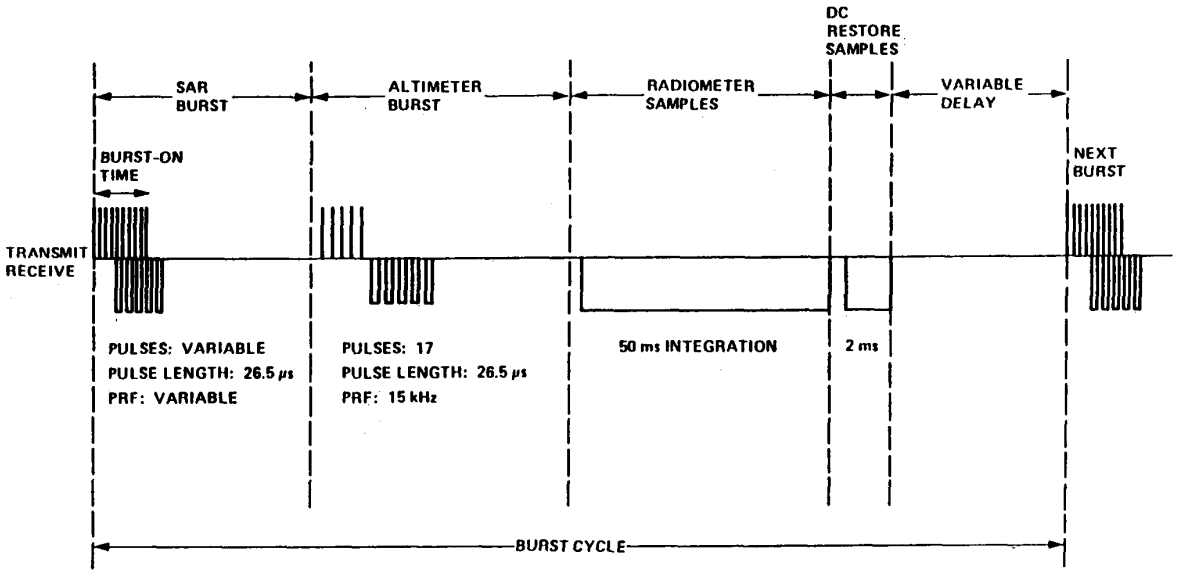

Fig. 2. MGN burst cycle timing.

between pulses, a factor of 1.25; 2) the radar is operated in the burst mode, a factor reduction of 9; and 3) a block adaptive quantizer is used, a factor of 4. The detailed design and implementation of the block adaptive quantizer is described in the following sections.

IV. MGN Radar Block Adaptive Quantizer (BAQ) Design

The following topics are discussed in this section: A) The quantizer model and quantization levels of the BAQ; B) the echo statistics of the radar echo returns; C) the expected power of the echo returns; D) the block estimation of the echo statistics; E) a description of the 2-bit quantizer; and F) the delayed application of the echo statistics.

A. Quantizer Model and Quantization Levels

The goal of adaptive quantization is to provide effective data compression of a signal source with time-varying parameters. An adaptive quantizer estimates the statistics of the source and attempts to match the quantizer to the observed time-varying statistics. In the approach taken to design the adaptive quantization scheme, the model shown in Fig. 3 was used. The statistics of a block of incoming data samples are estimated and a quantizer which is optimized for that source model is selected for quantization of that block of data. An understanding of the source statistics is therefore paramount in the design of an optimal quantizer. The reconstruction of the data samples is also an issue in the efficient mechanization of the quantization scheme. These issues and others are discussed in the following sections.

In a data rate limited system the selection of the number of levels of quantization is a trade-off between the range resolution (or pulse bandwidth) and performance of the quantizer (quantization noise). The range bandwidth determines the sampling rate of the echo returns and therefore affects the data rate. In addition, the performance of the quantizer affects the noise in the digital data and, therefore, the image quality. The decision to use a 2-bit converter in the SAR system was based on a balance of these two factors. In an earlier design of the system [3], a combination of the radar bandwidth of 1.13 MHz and a 3-bit converter produced a ground range resolution of 225 m at low altitudes and a converter quantization SNR of approximately 14 dB. In the present design of the SAR system [4] a radar bandwidth of 2.26 MHz and a 2-bit converter were settled upon for an improvement of the ground range resolution and a converter with a lower SNR. At low altitudes the ground range resolution became 120 m with a converter SNR of 8.7 dB. Based upon the performance of the 2-bit converter, the thermal SNR of the system was then chosen to be at least 8 dB. From simulations using real SAR data with this 2-bit converter and images with more than four looks, higher values of thermal SNR did not enhance the visual-image interpretation, and lower values degraded the images. Thus the

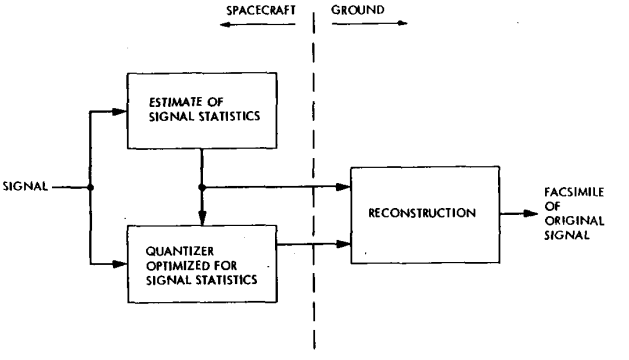

Fig. 3. Adaptive quantizer model.

thermal SNR of the system is compatible with the converter performance, and the system SNR which includes the above noise sources is approximately 5 dB.

B. MGN Radar Echo Statistics

In the MGN radar the radar echo is downconverted to baseband and split into I and Q components. These components are then digitized separately by two 8-bit A/D converters. The statistics of a block of these 8-bit data samples are computed and used to control the coding of a subsequent block of 8-bit data samples into 2 bits. The statistics of the I and Q data can be assumed to be Gaussian, with zero mean and unknown average power. A brief examination of the statistics of this source model is given here.

The radar returns are a superposition of responses of many small scatterers. The coherent radar return $A(x, y, z)$ at observation point (x, y, z) is written as

$$A(x, y, z) = \sum_{k=1}^{N_s} a_k e^{j\phi_k}$$

where $A(x, y, z)$ is represented as the sum of many elementary phasor contributions due to the independent scatterers, a_k is the reflectance amplitude, and ϕ_k is the phase delay which is a function of radar wavelength and path distance and is independent of a_k. Thus the elementary phasors can be assumed to have the following properties:

- The amplitude a_k and the phase ϕ_k are statistically independent of each other and of the amplitude and phase of all other elementary phasors.
- The phases ϕ_k are uniformly distributed on the interval $[-\pi, \pi]$ (the scatterers have an unknown range and the SAR resolution is much greater than the radar wavelength).

From these assumptions it can be shown that the real and imaginary parts of the complex signal have zero means, identical variances, and are uncorrelated [11], [12]. Due to the large area encompassed by the antenna footprint, the number of elementary phasor contributions can be considered to be extremely large; the real and imaginary parts of the reflected signal are therefore sums of a very large number of independent random variables. It follows from the central limit theorem that as $N_s -> \infty$, real and imaginary parts are asymtotically Gaussian with unknown variances.

C. Expected Power Variations of Echo Returns

An understanding of the power variations of the returns gives a basis for the design of the block size required to estimate the control statistics of the quantizer. The echo returns from a pulse are due to the convolution of the code with individual scatterers and have correlation properties of the coded pulse (a length of 60 biphase modulated code). The biphase code is chosen such that its autocorrelation function has a peak at zero and falls off to a low

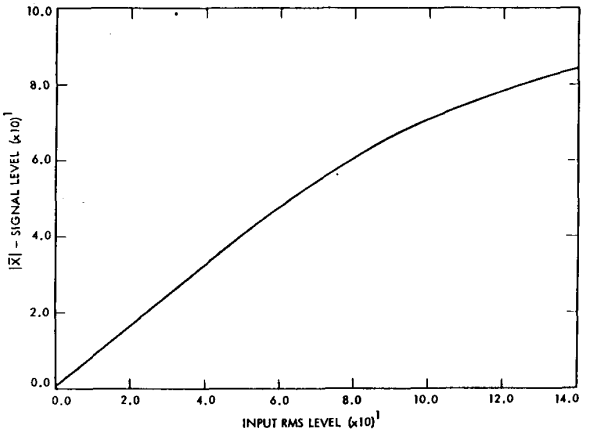

Fig. 4. Mapping of RMS input to magnitude statistics. The inverse mapping provides the estimate of the input power.

value for the time delay of a one-code bit or more; therefore successive range samples are uncorrelated but have the same expected power. Another factor which affects the return power is the antenna pattern—it weighs the returns as a function of range. Thus samples in a small neighborhood of the same transmit pulse have the same expected power return, but the coherent returns are uncorrelated. Moreover, the power changes are slowly varying.

The variation of the returns from pulse-to-pulse is also of importance. Analogous with range, coherent returns separated by a few pulses are essentially uncorrelated but have the same expected power due to the following reasons: During the collection time of the SAR burst, the expected power of a sample corresponding to a fixed range is approximately constant even in the presence of the most extreme range walk (due to target-sensor motion). The range walk more severely affects the variations over a time period from burst-to-burst. During this period the illumination footprint has moved in the cross-range direction from 0.075 to 0.175 beamwidths, and the range window has moved due to a range walk from 0 to 8 range samples. Since the returns are the result of the returns of the coherent sum of scatterer returns over the cross-range antenna-beam extent and the pulse duration of 60-range samples, the burst-to-burst variations in the expected power is also quite small.

In summary, the SAR signal statistic is Gaussian, with the variation in power of the return being a slow function of range, pulse number, and also from burst-to-burst returns. These statistics are the basis for the BAQ design.

D. Block Estimation of Control Statistics

The quantizer is controlled by the statistics of the incoming signal. Since the signals in both the I and Q channels are Gaussian with a zero mean, the distribution can be specified with a single parameter. The statistic selected to characterize this parameter is the average signal mag-

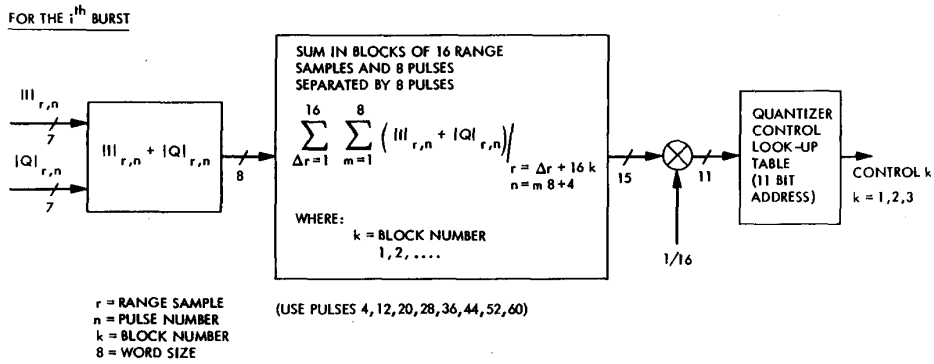

Fig. 5. Computation of magnitude statistic.

nitude, instead of the average signal power. If the outputs of the 8-bit A/D are used to generate this statistic, the average signal magnitude (for a zero-mean Gaussian signal) can be written as

$$\overline{|I|} = \overline{|Q|} = 2 \sum_{n=0}^{N-1} (x_n + 1/2) \int_{x_n}^{x_{n+1}} p(x)\, dx$$

and

$$p(x) = \frac{1}{\sqrt{2\pi\sigma}} e^{-x^2/2\sigma^2}$$

where x_n is the maximum average signal magnitude, x_i is the transition points of the 8-bit A/D, and σ is the standard deviation of the input signal to the A/D. Simplifying as follows:

$$\overline{|I|} = \overline{|Q|} = 127.5 - \sum_{n=0}^{127} \operatorname{erf}\left(\frac{n+1}{\sqrt{2}\sigma}\right) \qquad (1)$$

it can be seen that $\overline{|I|}$ approaches 0.5 as the input signal power goes to zero, and approaches 127.5 as the signal power goes to infinity. This equation provides the mapping of the RMS input level (σ) to the average magnitude statistics. Fig. 4 shows a plot of the magnitude statistic as a function of input signal power. Thus even when the instantaneous input power is large and the A/D saturates, the magnitude statistic still provides a good estimate of the signal power. The performance difference between using this statistic and the direct estimation of the average signal power is small. However, the reduction in hardware complexity more than justifies this approach.

The slowly varying echo power in range and from pulse-to-pulse makes possible the block estimation of the magnitude statistic. Fig. 5 shows the computation of this magnitude statistic using blocks of data samples. For each group of 16 range samples the magnitude of the I and Q samples are added together for 8 pulses (selected at every eighth pulse). Thus the statistic for each block of 16 range samples consists of the sum of 256 samples from the 8-bit A/D. To account for edge effects, the last block (which may have fewer than 16 additional range samples) uses the last 16 range samples to form the statistic. Using the statistic described, the quantizer control (threshold) is found using a look-up table. This is performed by dividing the statistic by 16 and forming an 11-bit word to be used as an address for a 4K ROM whose output is a 8-bit word. The ROM contains the map from the statistic to the control parameter of the quantizer. The mapping selected minimizes the distortion of the quantizer (both quantization and saturation effects). The 8-bit quantizer control for each group of 16 range samples is encoded in the burst header and is transmitted for use in the decoding process.

E. 2-bit Nonuniform Quantizer

The next element in the BAQ is the quantizer. Within the quantizer each 8-bit data sample is encoded into 2 bits. One bit is the sign bit and the other bit indicates the signal level. The signal-level bit indicates whether the magnitude of the I or Q sample is above or below a threshold. The value of this threshold is described above. For a 2-bit quantizer this threshold represents the transition point that is optimally placed in an ensemble of input data with a Gaussian probability density such that the distortion in the reconstructed data is minimized in a mean-square-error sense. The four output states of the converter are the centroids of the areas between zero and the transition points and the centroids of the areas between the transition points and infinity (see Fig. 6). The signal-to-noise ratio of the output of the quantizer versus the input signal is shown in Fig. 7. It can be seen that an SNR of 8.7 dB can be achieved if an accurate estimate of the input statistic is available. The calculation of the optimal transition points as well as the output states are well documented in Collins and Sicking [13].

In the decoding process, the I and Q samples are reconstructed using the threshold information and the encoded 2-bit data of each block. For a given block of 2-bit data, the floating point I/Q samples y_n are reconstructed by

$$y_n = \begin{cases} (sign) \times 0.52 \times Th & \text{magnitude bit} = 0 \\ (sign) \times 1.73 \times Th & \text{magnitude bit} = 1 \end{cases}$$

where the *sign* is indicated by the sign bit and *Th* is the threshold value downlinked in the burst header. The coef-

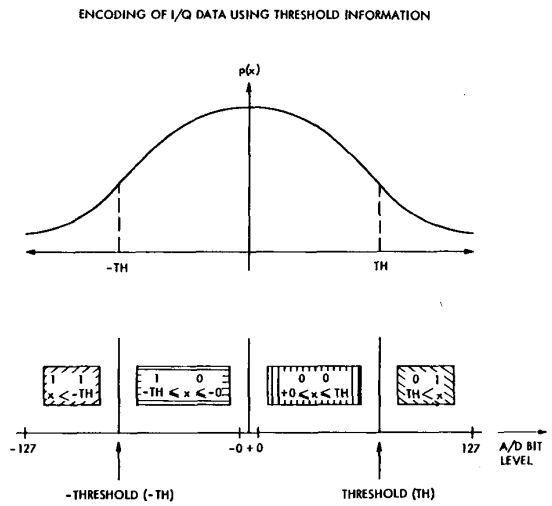

Fig. 6. Transition points of a 4-state output quantizer.

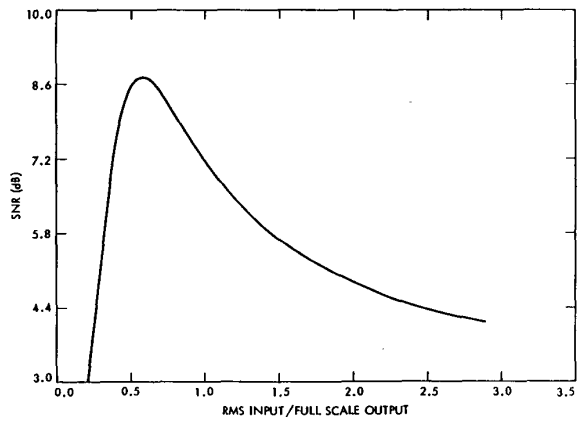

Fig. 7. Signal-to-noise ratio of output versus input signal level expressed as a fraction of full-scale output.

ficients 0.52 and 1.73 are the optimal output levels of a nonuniform 2-bit quantizer whose input is normally distributed with zero mean and unit variance. The decoding of the 2-bit data into the 4 output states is shown in Fig. 8.

F. Delayed Application of Thresholds

During the operation of the radar the thresholds that are used to encode the radar returns from a given burst are those generated during a previous burst (see Fig. 9). This is possible due to the small variation in the expected power of the returns from burst-to-burst (see discussion above). Again, this is done to reduce the complexity of the hardware. A maximum of 24 thresholds can be generated during each burst.

V. Implementation of BAQ in Hardware

A functional block diagram of the hardware is shown in Fig. 10. The BAQ hardware consists of the threshold and bit select circuits.

2 bit DATA	RECONSTRUCTED VALUE
0 0	0.52 Th
1 0	-0.52 Th
0 1	1.73 Th
1 1	-1.73 Th

Th = THRESHOLD FROM BURST HEADER

Fig. 8. Decoding of 2-bit data.

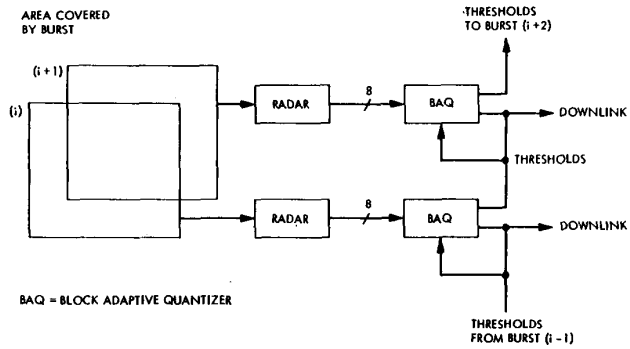

Fig. 9. Delayed application of thresholds.

In the threshold circuit the sum of the magnitude of 256 I and Q samples from the 8-bit A/D is used to provide an estimate of the signal-level statistic. As described previously, these samples are made up of blocks of 16 range samples from 8 pulses (taken at every 8th pulse). Using this statistic the quantizer control is found using a look-up table. This is performed by dividing the statistic by 16 and forming an 11-bit word to be used as an address for a 4k ROM whose output is a 7-bit word. The ROM contains the map from the statistic to the control of the quantizer (a mechanization of (1)). Hence a total of 127 control thresholds are available to adapt the quantizer to the time-varying statistics. This gives the BAQ a possible dynamic range of approximately 39.5 dB at a minimum 8.5-dB signal-to-distortion noise ratio (see Fig. 11). This 7-bit quantizer control or threshold for each block is encoded in the burst header and downlinked for use in the reconstruction process.

The bit selector circuit uses the thresholds generated during the previous burst to encode the I and Q data samples into 2 bits. The sign bit of each 8-bit data word from the A/D is carried around the bit selector circuit and is always one of two downlinked bits. The 7-magnitude bits of the data samples are compared to the 7-bit threshold bits. If the sample's magnitude is greater than the threshold, a "one" is downlinked; otherwise, the second data bit is "zero."

VI. Simulation Results

This section presents a set of the results of the simulations designed to test the BAQ.

First, the step response (a 30-dB step, Fig. 12) of the BAQ was analyzed. This was generated by the convolution of the step with the MGN radar biphase code; by

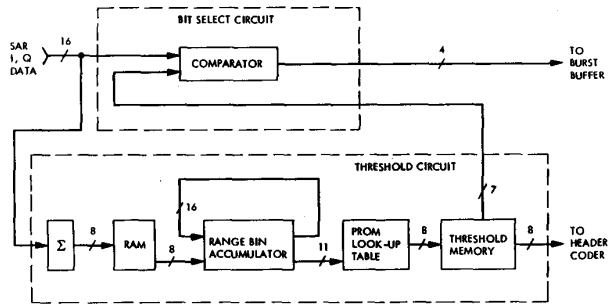

Fig. 10. Functional block diagram of the BAQ.

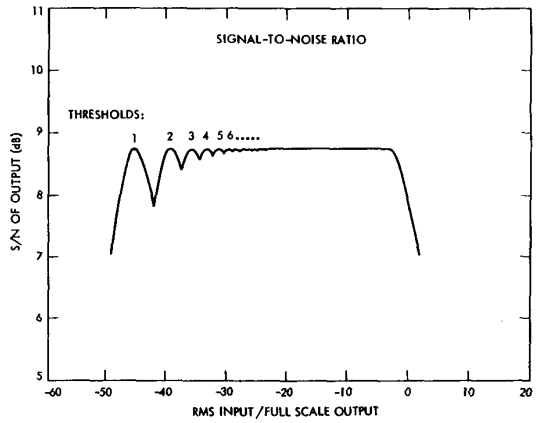

Fig. 11. Predicted performance of the BAQ.

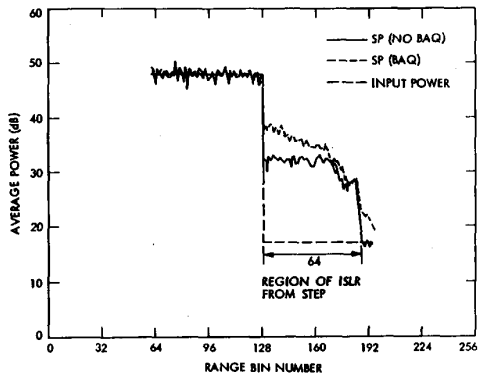

Fig. 12. Step response of the BAQ.

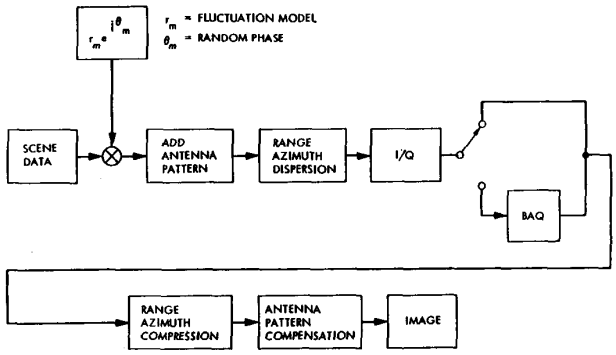

Fig. 13. Simulation approach.

quantizing the data samples with the BAQ; and by decoding the data samples and pulse compressing the data. The input power and the signal power (SP) of the response with and without the BAQ are shown in Fig. 13. As expected, the output power turns out to be very close to the input power in the region of high reflectivity. The difference in the low reflectivity area (within 64 range bins from the transition point) can readily be explained as power leakage from the high reflectivity area resulting from finite-range side lobes. With the BAQ in the simulation the total average output power is higher than that measured in the previous case without the BAQ since the output power includes signal power plus quantization noise power due to the BAQ. This can be confirmed by comparing the two power curves in Fig. 14. The peak of the main lobe to the highest side lobe ratio (PSLR) of the compressed pulse is approximately 22 dB (which is the expected PSLR performance of the biphase code) and the quantization SNR of the converter is 8.5 dB.

Next, to investigate the visual effect of the BAQ on SAR imagery and to simulate SAR burst-mode BAQ operation, the approach shown in Fig. 13 is used. The following steps were used to generate the 2-bit I and Q data from magnitude images and were then recompressed to form SAR imagery:

1) The scene magnitude data are first degraded with a fluctuation model (Rayleigh magnitude fluctuation and a random phase).

2) The data are then weighted with the antenna pattern.

3) The data are then dispersed in range by the MGN range code and dispersed in azimuth (i.e., convolution with expected range/azimuth response).

4) The data are either quantized to 8 bits or coded to 2 bits using the BAQ. This provides the basis of comparison between the two modes of quantization.

5) The 2-bit data are reconstructed and processed (i.e., range and azimuth compressed) and compared to the processed 8-bit data.

The simulation results are shown in Figs. 14 and 15. Fig. 14 shows the results of a simulation using simulated terrain data and Fig. 15 shows the results of a simulation using an actual SAR image with more than 20 looks or with very low speckle noise. The 3 images in each figure are the original image, the image formed using a uniform 8-bit quantizer, and the image formed using the BAQ, respectively. Each image is 300 × 400 pixels with a resolution of 150 m and a pixel spacing of 75 m simulating the actual resolution and spacing of the Magellan radar. The simulated images have four looks each. The visual

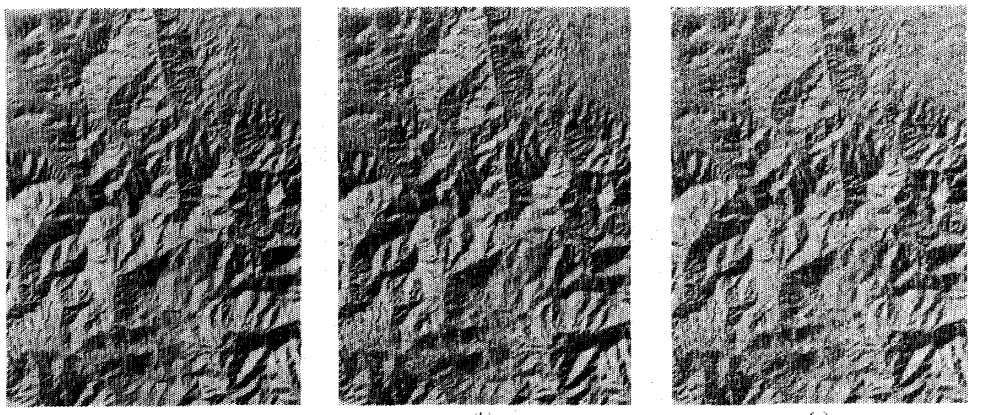

(a) (b) (c)

Fig. 14. Simulation results. (a) Simulated terrain data. (b) Image formed using an 8-bit uniform quantizer. (c) Image formed using the BAQ.

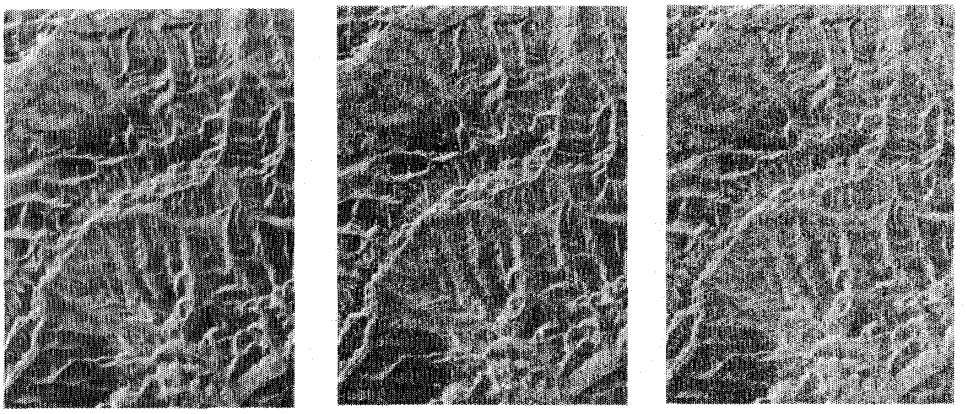

(a) (b) (c)

Fig. 15. Simulation results. (a) SAR image. (b) Image formed using an 8-bit uniform quantizer. (c) Image formed using the BAQ.

quality of the images formed using the BAQ can be compared to the image formed using a full 8-bit quantizer.

As observed in [1] and as indicated in the simulated image data, the general noise level in the imagery generated using data quantized by the BAQ can be seen to be higher than that generated by using an 8-bit quantizer. Thus an expected degradation in the SNR can be seen in the simulated-image data. The quality of the images generated by the Magellan SAR and its effect on analysis of surfacial features on Venus can be found in [14]. As a final remark, the design of an SAR system consists of the balance of many mission-related constraints. This paper illustrated one approach to the optimization of data quality as related to the limitations of the communication bandwidth between the sensor and Earth ground stations.

VII. Summary

An adaptive quantization scheme which will be used in the MGN Venus mission in 1989 has been presented. The theory behind the quantization model is given and the implementation is described. Simulations have demonstrated the expected performance of the BAQ. This adaptive quantizer design allowed a data rate reduction which satisfied the hardware constraints and also the radar system requirements.

Acknowledgment

The authors wish to thank D. Evans and K. Cho and especially H. Nussbaum of the Radar Systems Group, Hughes Aircraft Company, and T. Joo of the Jet Propulsion Laboratory for their valuation contributions to the

analysis and development of the Magellan Radar Block Adaptive Quantizer.

REFERENCES

[1] R. G. Lipes and S. A. Butman, "Bandwidth compression of Synthetic Aperture Radar imagery by quantization of raw radar data," *SPIE*, vol. 119, pp. 107, 114, 1977.

[2] T. H. Joo and D. Held, "An adaptive quantization method for burst mode Synthetic Aperture Radar," presented at the Int. Radar Conf., Arlington, VA, May 6-9, 1985, pp. 385-390.

[3] W. T. K. Johnson, "The Venus Radar Mapper: Radar system design for highly elliptical orbits," in *Proc. IGARSS '84* (Strasbourg, France), 1984.

[4] W. T. K. Johnson and A. T. Edgerton, "Venus Radar Mapper (VRM): Multimode radar system design," *SPIE*, vol. 589, pp. 158-164, 1985.

[5] S. S. Dallas, "The Venus Radar Mapper mission," presented at the 25th IAF Congress, Lausanne, Switzerland, Oct. 1984, Paper IAF-84-196.

[6] J. H. Kwok and S. S. Dallas, "Mission and trajectory design for a Venus Radar Mapper mission," presented at the AAS/AIAA 21st Aerospace Sci. Meet., Reno, NV, 1983, Paper AIAA-83-0348.

[7] M. I. Skolnik, *Radar Handbook*. New York: McGraw-Hill, 1970.

[8] L. Porcello, N. G. Massey, R. B. Innes, and J. M. Marks, "Speckle reduction in Synthetic Aperture Radars," *J. Opt. Soc. Amer.*, vol. 66, pp. 1305-1311, Nov. 1976.

[9] K. Tomiyasu, "Tutorial review of Synthetic Aperture Radar (SAR) with applications to imaging of the ocean surface," *Proc. IEEE*, vol. 66, pp. 563-583, May 1978.

[10] J. J. Kovaly, Ed., *Synthetic Aperture Radar*. Dedham, MA: Artech, 1976.

[11] J. W. Goodman, "Statistical properties of speckle patterns," in *Laser Speckle and Related Phenomena: Topics in Applied Physics*, vol. 9, J. Dainty, Ed. New York: Springer-Verlag, 1975, pp. 9-75.

[12] F. T. Ulaby, R. K. Moore, and A. K. Fung, *Microwave Remote Sensing: Active and Passive*, vol. 2. New York: Artech, 1986.

[13] F. A. Collins and C. J. Sicking, "Properties of low precision analog-to-digital converters," *IEEE Trans. Aerosp. Electron. Syst.*, vol. AES-12, pp. 643-646, Sept. 1976.

[14] R. E. Arvidson *et al.*, "Construction and analysis of simulated Venera and Magellan images of Venus," *ICARUS*, vol. 75, pp. 163-181, 1988.

Ronald Kwok (S'82-M'84) received the B.Sc. (summa cum laude) degree from Texas A&M University, College Station, in 1976, and the Ph.D. degree from Duke University, Durham, NC, in 1980. He was a Postdoctoral Fellow at the University of British Columbia, Vancouver, BC, in 1981.

He was with MacDonald Dettwiler and Associates in Richmond, BC, where he worked on algorithms for Landsat and Radarsat ground-data systems. In 1985 he joined the Radar Science and Engineering Division at the Jet Propulsion Laboratory in Pasadena, CA, where he developed techniques for the analysis of SAR imagery and served in a radar-system engineering capacity on the Magellan and Alaska SAR facility projects. He is currently Group Leader in the SAR Systems Development and Processing Group, responsible for the research and development of post-processing and analysis techniques for SAR-image data.

Dr. Kwok is a member of Tau Beta Pi, Phi Kappa Phi, and Eta Kappa Nu.

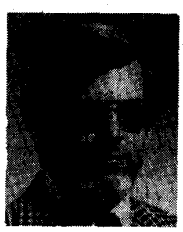

William T. K. Johnson was born in Seoul, Korea, in 1938. He received the B.S. degree in physics from the University of North Carolina at Chapel Hill in 1962, and the M.S. degree in atmospheric physics and Ph.D. degree in nuclear physics from the American University, Washington, DC, in 1966 and 1970, respectively.

He worked at the Harry Diamond Laboratories, the Rand Corporation, and the General Research Corporation before coming to the Jet Propulsion Laboratory, Pasadena, CA, in 1975, where he has worked on various synthetic aperture radar programs, including Seasat-SAR, Shuttle Imaging Radar—A, and the Magellan mission to Venus for which he is presently the Radar System Chief Engineer.

Dr. Johnson is a member of the American Physical Society.